

High Current ESD Test of Advanced Triple Junction Solar Array Coupon

Kenneth H. Wright, Jr., Todd A. Schneider, *Member, IEEE*, Jason A. Vaughn, Bao Hoang, *Member, IEEE*, Frankie Wong, *Member, IEEE*

Abstract— Testing was conducted on an Advanced Triple Junction (ATJ) coupon that was part of a risk reduction effort in the development of a high-powered solar array design by Space Systems/Loral, LLC (SSL). The ATJ coupon was a small, 4-cell, two-string configuration that has served as the basic test coupon design used in previous SSL environmental aging campaigns. The coupon has many attributes of the flight design; e.g., substrate structure with graphite face sheets, integrated by-pass diodes, cell interconnects, RTV grout, wire routing, etc. The objective of the present test was to evaluate the performance of the coupon after being subjected to secondary arc testing at two string voltages (100 V, 150 V) and four array currents (1.650 A, 2.000 A, 2.475 A, and 3.300 A). An external test circuit, unique to SSL solar array design, was built that simulates the effect of missing cells and strings in a full solar panel with special primary arc flashover circuitry. A total of 73 primary arcs were obtained that included 7 temporary sustained arcs (TSA) events. The durations of the TSAs ranged from 50 micro-seconds to 2.75 milli-seconds. All TSAs occurred at a string voltage of 150 V. Post-test Large Area Pulsed Solar Simulator (LAPSS), Dark I-V, and By-Pass Diode tests showed that no degradation occurred due to the TSA events. In addition, the post-test insulation resistance measured was > 50 G-ohms between cells and substrate. These test results point toward a robust design for application to a high-current, high-power mission.

Keywords—*Photovoltaic Cell Testing; Electro-Static Discharge Testing; High Power Solar Array*

I. INTRODUCTION

In order to provide power for increased payload sophistication and/or increased number of payloads, satellite power systems are motivated to increase photovoltaic array (PVA) string voltages and string currents. These voltages and currents may exceed 100V and 1 Amp, respectively. The International Space Station PVAs use 160V for power

generation [1]. Recently, Cho et al. [2] reported a nanosatellite test flight demonstrating 350 V operations.

When power increases on the satellite, there is an increased risk for problems, notably sustained arcs. Bodeau [3] surveyed a large amount of ground test data and compared that with a large amount of vacuum arc data to derive a safe operating region: string currents < 1 A for < 200 V. For future high power satellite power systems, careful consideration should be given to design and that design should be verified through adequate testing.

Space Systems/Loral, LLC (SSL) is developing a high power satellite bus system for future applications. Coupon-level tests were performed at the Marshall Space Flight Center (MSFC) to investigate PVA design robustness for voltages > 100 V and currents > 1 A. SSL and MSFC have several years of partnership in combined space environment testing to qualify various aspects of SSL PVA design [4] - [7]. For the results reported in this paper, only induced electrostatic discharge (ESD) testing was performed. The protocol for testing (both arc inception and secondary arc testing) was based on the recent ISO standard [8].

II. TEST PLAN

The objective of the ESD testing was to evaluate performance of a single coupon in configurations at two string voltages (100V, 150V) and four string currents (1.650A, 2.000A, 2.475A, and 3.300A). A cumulative total of 70 arcs were planned. See Table I for the delineation of arcs per case and the sequence of test progression. The test coupon underwent no environmental aging at MSFC. That is to say, no radiation, UV, thermal cycling, and/or ion erosion environments were applied before testing. The test condition was ambient temperature in the inverted gradient potential case. The coupon tested at MSFC had undergone previous secondary arc testing at the Kyushu Institute of Technology (KIT). In testing at KIT, a total of 71 arcs were induced over three voltages (100V, 120V, 150V) and two string currents (1.00A, 1.65A). Hoang et al. [9] report the results of the KIT testing. Coupon D in Hoang et al. [9] is the same coupon that was tested at MSFC.

The test article was a small, four cell Advanced Triple Junction (ATJ) coupon. This coupon was one from a series of coupons produced from a common manufacturer that underwent testing both at KIT and at MSFC. Each individual cell assembly contains a silicon bypass diode. Two

The work at the NASA/Marshall Space Flight Center was performed under Space Act Agreement (SAA8-084200) with Space Systems/Loral, LLC. The work of K. H. Wright, Jr. was supported by NASA through a Cooperative Agreement with the University of Alabama-Huntsville (NNM11AA01A).

Kenneth H. Wright, Jr. is with the Center for Space Plasma and Aeronomic Research, University of Alabama-Huntsville, Huntsville, AL 35899, USA (e-mail: Ken.Wright@uah.edu)

Todd A. Schneider and Jason A. Vaughn are with the NASA/Marshall Space Flight Center, Huntsville, AL 35812, USA (e-mail: todd.a.schneider@nasa.gov; jason.a.vaughn@nasa.gov)

Bao Hoang and Frankie Wong are with Space Systems/Loral, LLC, Palo Alto, CA 94303, USA (email: Bao.Hoang@sslmda.com; Frankie.Wong@sslmda.com)

independent “strings” of cells are formed by connecting two cells together in series to form a single string. The string layout on the coupon represents a typical string layout on a flight solar array panel. As a part of the SSL ESD mitigation design, the cell laydown included room-temperature vulcanizing (RTV) adhesive grout applied to interconnects, busbars, and the gap between cell strings. There is no intentionally placed RTV between cells in the same string.

TABLE I. NUMBER OF ESD ARCS REQUIRED

String Potential (V)	String Current (A)	Number of ESD Arcs Required
100	1.650	5
150	1.650	5
100	2.000	10
150	2.000	10
100	2.475	10
150	2.475	10
100	3.300	10
150	3.300	10
Arc Summary Total		70

Figure 1 shows the coupon layout. The string on the left side of the coupon is string 1 and biased at the “String Potential” voltage noted in Table I. The string is on the right side of the coupon is string 2 and is the reference side for the voltage bias of string 1. Each coverglass has an anti-reflective coating. Both strings are mounted on a Kapton sheet which is applied to a substrate structure composed of an aluminum honey-comb core with graphite face sheets. The substrate is constructed with holes in all four corners which provide a pass-through for the string wires and can be used for sample mounting. An insulating bushing is inserted in each corner hole to help isolate the pass-through wires from the grounded honey-comb structure. The size of the coupon and the limitation to a 2x2 cell format was dictated by the original 25.4 cm diameter illumination region in the MSFC radiation target chamber. A recent upgrade to the MSFC radiation target chamber allows for an illumination region of 76.2 cm in diameter.



Fig. 1. Picture of test coupon. The coupon has been configured into two strings with each string composed of two cells. [4]

III. TEST SETUP

A. Experimental Arrangement

Testing was carried out in one of the vacuum chambers that reside in the NASA/MSFC Space Environment Effects Facility. The details of this particular vacuum chamber have been described elsewhere [4] but basic information is included here. The chamber is 2.1 m long by 1.2 m diameter with cryo-pumping capability. Base pressure reaches $\leq 1.3 \times 10^{-4}$ Pa ($\leq 1 \times 10^{-6}$ torr). A liquid nitrogen shroud of dimension 1.2 m long by 1.11 m diameter resides at one end of the chamber while a 100-keV flood gun is mounted on the other end of the chamber. Electron beam energies used in this test were ≤ 6 keV at current densities of 1 -2 nA/cm² with $\sim 90\%$ uniformity across the coupon. All testing in this study was performed at room temperature. A 2-D stage allows movement of a Faraday Cup and Trek probe to either measure the electron beam flux or measure the coupon surface potential. An array of Tektronix oscilloscopes records diagnostic signals from the external test circuit and a video camera with both VCR and DVR recording systems (30 frames/sec) capture visual evidence of arcs.

B. Arc Inception Voltage Test

A dedicated control rack houses a high voltage power supply to bias the coupon and several current probes (Pearson Coils) to capture movement of charge in response to an arc. A small (few nano-Farad) capacitor supplies charge for primary arc generation. The size of this capacitor is enough to allow for visual identification of the arc location. Fig. 2 shows the schematic of the arc inception voltage setup. The network of capacitors inside the chamber simulates the capacitance of missing cells and the capacitance of cells to substrate in the flight architecture. For arc inception voltage testing, these capacitors are not needed but their presence allows continuing to secondary arc testing without a vacuum break.

Testing was performed in the inverted gradient condition; i.e., the cell coverglass was more positive than the substrate. Initiation of the arc is caused by sequentially manipulating the electron beam flux and illumination time on the coupon. Measurement of the surface potential after each electron beam exposure allows a fairly precise way of determining the arc inception voltage. Details of the electron beam exposure method can be found in Wright et al. [4].

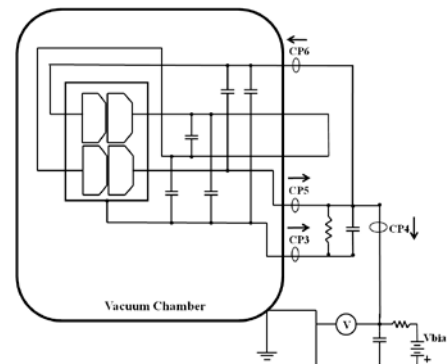


Fig. 2. Arc inception voltage test circuit. “CP” indicate location of current probe and “V” indicates location of the HV probe. [4]

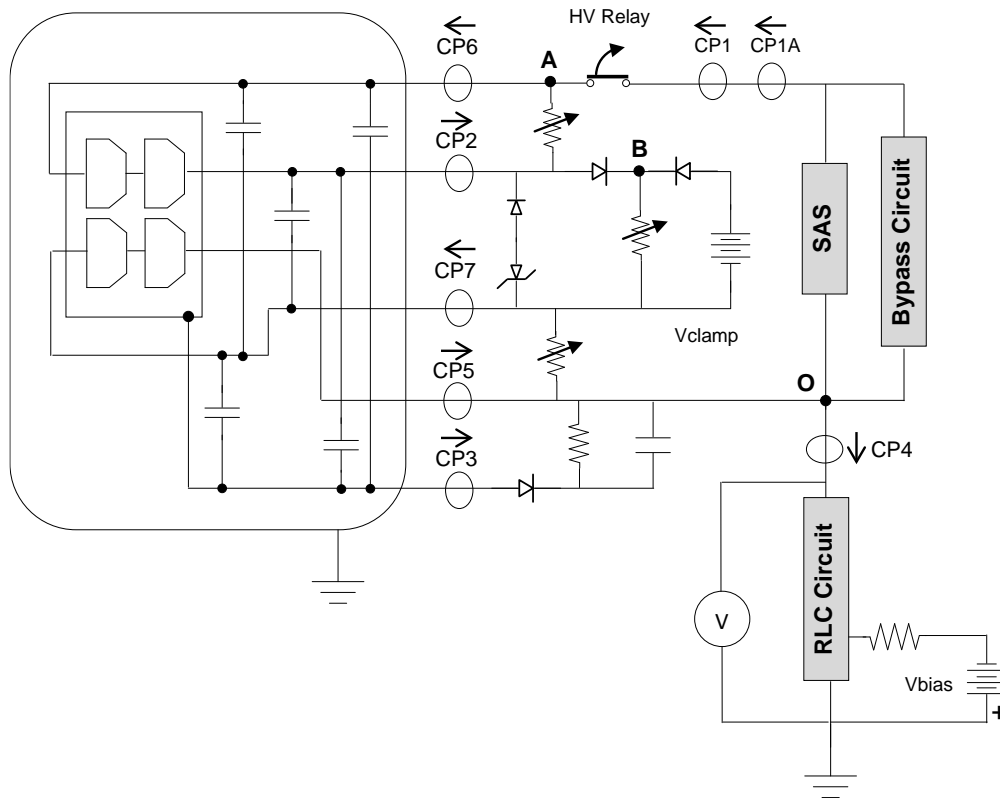


Fig. 3. Secondary arc test circuit. “CP” indicates location of current probe and “V” indicates location of the HV probe. “A” and “B” indicate voltage measurement locations referenced to point “O.” SAS is the Solar Array Simulator. [7]

C. Secondary Arc Test

A separate equipment rack houses the SSL specialized secondary arc test circuit. Various circuit elements are included to allow simulation of the effects of a whole array panel while using only a small coupon. Key to this special setup is the primary arc (PA) pulse generation circuit. It is comprised of a resistor-inductor-capacitor (RLC) network to produce a pulse of amplitude (28 A) and duration ($\sim 190 \mu\text{s}$) for the coverglass flashover.

The PA pulse used in this test campaign is described by Wright et al. [4] [7] and Hoang et al. [9]. For continuity of setup between this test and previous testing [4] [7] [9], the PA circuitry was kept in place. A key assumption in the derivation of this PA pulse was a constant plasma speed of 10 km/s. Recent work has been performed to delve deeper into PA characteristics [10-13]. A round robin test effort [14-16] is presently underway with the goal of reaching agreement concerning the nature of PA pulse speed and shape. The authors realize that the PA pulse used in this test is different from the current trend of a lower amplitude and longer pulse.

The test circuit is shown in Fig. 3. Of special note is an arc interruption circuit that forces a HV relay to open a switch approximately 3 milli-sec after arc initiation. This feature is used to prevent a sustained arc from causing ultimate coupon failure. The 3 milli-sec time value is arbitrary in that it was

chosen to be sufficiently longer than the primary arc pulse to allow any tendency for sustained arcing to develop ($> 1\text{ms}$) [17].

IV. TEST RESULTS

A. Arc Inception Voltage

Arc inception voltage was measured, as described in Section III B, before commencing secondary arc testing. A total of five arc events were acquired. The average arc inception value was $\sim 900 \text{ V}$. These measurements were obtained after 3 days under vacuum and at a background pressure of $1.07 \times 10^{-4} \text{ Pa}$ ($8 \times 10^{-7} \text{ Torr}$).

During the performance of the secondary arc testing, the arc inception voltage was not directly measured via the Trek probe location over the surface but inferred to increase as evidenced by the continual lowering of the electron beam energy required to induce an arc. For example, during the initial arc inception voltage testing the electron beam energy began at 6 keV and ended at $\sim 5 \text{ keV}$ (suggesting a $\sim 1000 \text{ V}$ arc inception voltage). As the final arcs were obtained in the 150 V/3.300 A case, it is inferred that the arc inception voltage was larger. The electron beam energy change in this case started at 6 keV and ended at $< 2.5 \text{ keV}$. However, the energy change noticed during the electron beam exposure sequence has only been qualitatively correlated with actual surface measurements.

It is speculated that the apparent increase in arc inception voltage resulted from surface modifications due to cumulative arc events over the course of this test and previous testing at KIT.

B. Secondary Arc

The test sequence was performed according to Table I starting with the lowest string voltages and currents and progressing to the highest string voltages and currents. Table II shows the as-run sequence. Three additional arcs were produced: two arcs were produced while measuring the coupon Arc Inception Voltage at the end of the testing and in one case the oscilloscopes were not ready. The occurrence of Temporary Sustained Arc (TSA) events is also noted in Table II. A TSA is defined as any secondary arc event that extends beyond the primary arc pulse of nominal 190 μs duration. Table III shows the duration beyond the primary arc for each of the seven TSA events.

TABLE II. AS-RUN ESD ARC DATA

String Potential (V)	String Current (A)	Number of ESD Arcs Acquired	Number of TSAs
100	1.650	5	0
150	1.650	5	0
100	2.000	10	0
150	2.000	10	1
100	2.475	10	0
150	2.275	10	2
100	3.300	12	0
150	3.300	11	4
Arc Summary Total		73	7

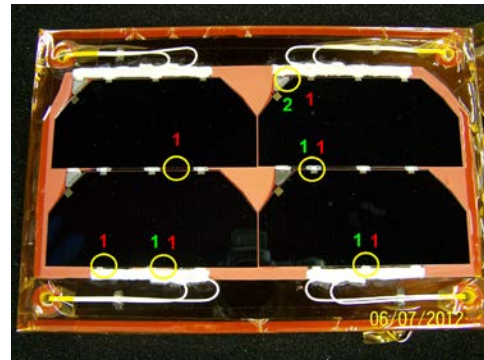
TABLE III. TSA OCCURRENCE CONDITION AND DURATION

String Potential (V)	String Current (A)	Duration (μs)
150	2.000	250
150	2.475	160
150	2.475	230
150	3.300	50
150	3.300	190
150	3.300	*
150	3.300	2750

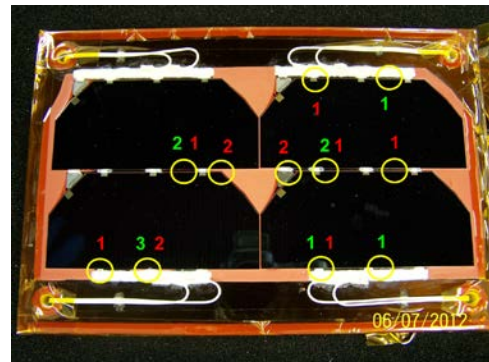
* No oscilloscope data available

the figure, preferential arc sites include bus bars, interconnects, and cell edges.

a.



b.



c.

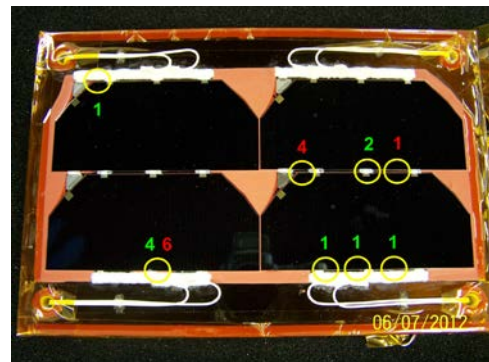


Figure 4 shows an arc site map for each of the four string current levels. The number of arc occurrences per location is noted on each figure and color coded as to voltage. As seen in

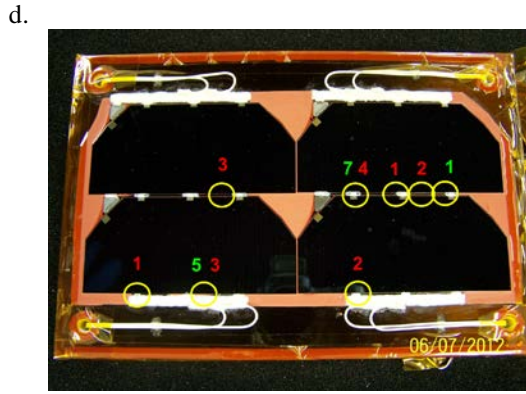


Fig. 4. Arc site locations. Each number by the circle indicates the number of events at that site. Green number is arc count at 100 V string voltage and red number is arc count at 150 V string voltage. The different sub-plots are for each string current tested: a. 1.650 A. b. 2.000 A. c. 2.475 A. d. 3.300A.

A picture of the longest duration TSA event at string voltage 150 V and string current 3.300 A is shown in Fig. 5. The current and voltage probe data for this event is shown in Fig. 6. The PA occurred on string 2 (see CP5 and CP7 in Fig. 6b) and jumped to string 1 to form the TSA. The inferred path of the SAS current, based on the current probe behavior, is overlaid in Fig. 5. The TSA ended upon the opening of the arc interruption switch – which may actually qualify this arc as a permanent sustained arc.

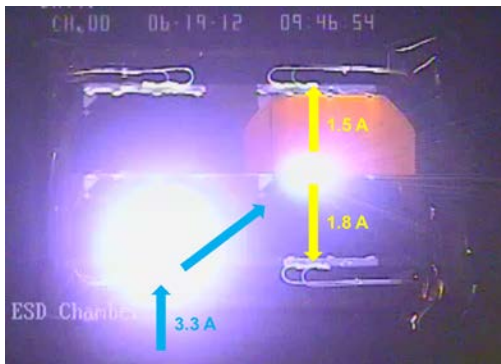


Fig. 5. Picture of the TSA event at 150 V and 3.300 A. The event duration was 2750 μ s. The event may have gone longer but was stopped by the arc interruption switch opening. The path for the SAS current is also shown.

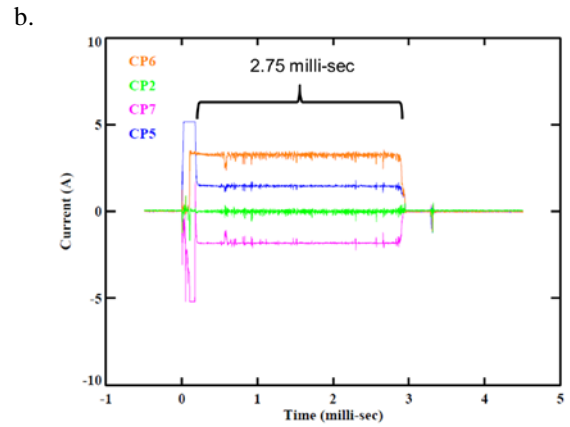
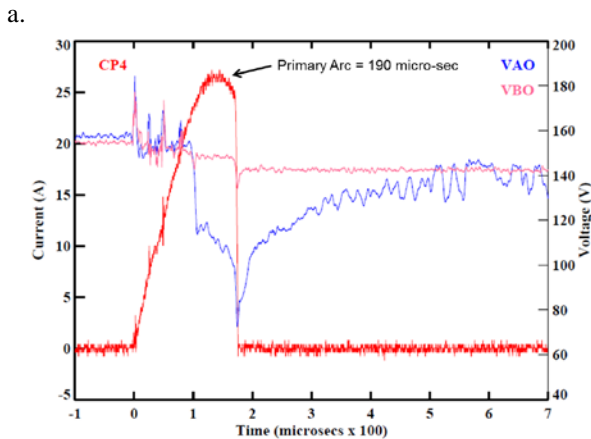
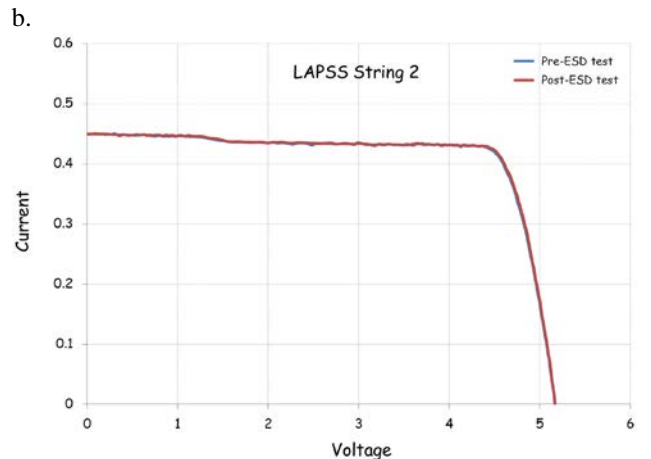
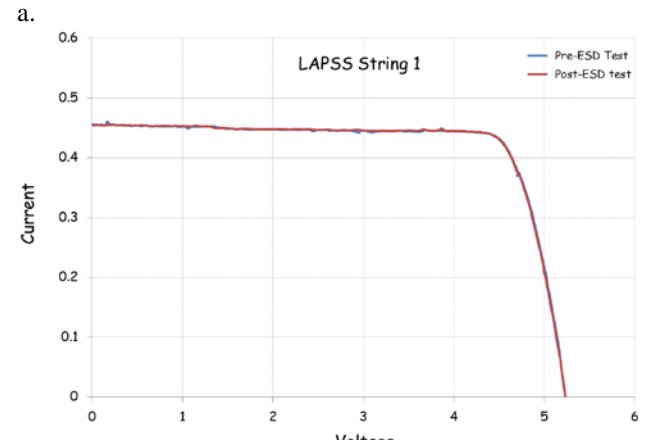


Fig. 6. Current and voltage probe data for the TSA event pictured in Fig.5. Refer back to Fig. 3 for map of CP layout. a. CP4 and voltage probe data. VAO, VBO refers to voltage difference between points A and O, B and O respectively. Refer to Fig.3. Time-base chosen to resolve primary arc pulse. b. Current probe data for each of the four cells on the coupon. Time-base chosen to capture any extended secondary arc activity. Amplitude chosen to resolve any SAS current flow between strings.

C. Functional Tests

The functional performance of the coupon was measured both before and after testing. The comparison results of Large Area Pulsed Solar Simulator (LAPSS), Dark IV, and By-Pass diode testing are shown in Fig.7. The LAPSS data provides the key performance data while Dark-IV and By-Pass diode test provide insight into subtle changes over time.



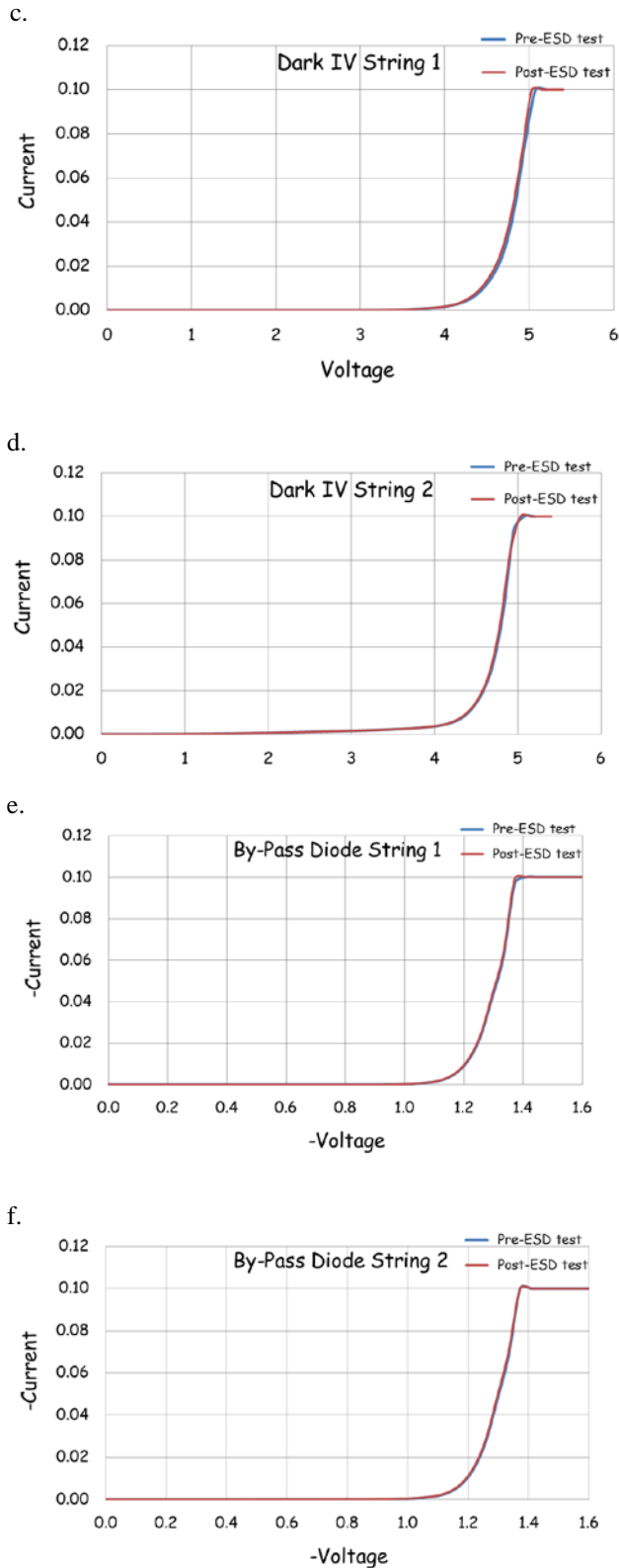


Fig. 7. Functional test data from before and after ESD testing. a. LAPSS String 1 b. LAPSS String 2 c. Dark-IV String 1 d. Dark-IV String 2 e. By-Pass Diode String 1 f. By-Pass Diode String 2

V. SUMMARY

ESD testing was performed on a basic SSL solar array architecture captured on a coupon that had no previously induced environmental aging (UV, radiation, and thermal cycling) with the exception of prior secondary arc testing. Coupon attributes included RTV applied to interconnects, busbars, and the gap between strings. Test parameters were chosen to anticipate the array bus voltages and currents that may be used in a future SSL array design for high power application. The voltage/current test parameters used here extend those used in the previous study of Hoang et al. [9]. The purpose of this test was to examine the present design susceptibility to high power operation. A total of 73 primary arcs were induced with seven TSA events observed. All TSA events occurred at 150 V over three different string currents (2.000 A, 2.475 A, and 3.300 A) with the number of TSA events increasing with increasing current level. For Coupon C and Coupon D (the same coupon tested at MSFC), whose test results are reported in Hoang et al. [9], a cumulative 132 primary arcs were induced with only two TSA events observed: one at 150 V/1.0 A and one at 150 V/1.65 A. To summarize the combined results from Hoang et al. [9] and this test, (1) no TSA events were observed for 100 V and currents < 3.300 A and (2) TSA events were observed for 150 V and at all currents tested ≥ 1.0 A with a greater chance for TSA occurrence at the larger currents (e.g., 3.300 A).

The duration of the TSA events in this test exhibit no discernible pattern. It is important to note that the longest TSA event was terminated via a pre-determined test circuit operation. Whether this event could have evolved into a sustained arc with significant damage to the coupon is uncertain. All functional test data obtained post-secondary arc testing indicated no degradation in cell performance. Insulation resistance measured post-ESD testing was > 50 G Ω between all cells and the substrate. In addition, microscopic examination of the coupon path between string 1 and string 2.

Based on the information published by Bodeau [3], the TSA occurrences observed in this test come as no surprise. These operational voltages and currents are in the high-risk zone as defined by Bodeau [3]. The present SSL design indicates robustness against some region of high power operation. But if power in the 150V/3A range is envisioned, further design and test work is needed, especially when the reality of environmental aging is considered [7]. Recent results from coupon tests with grouted, aged coupons [18-20] indicate that the threshold for sustained arcing is near 120 V/ 2.4 A.

ACKNOWLEDGMENT

The authors would like to acknowledge the following students for providing assistance in performance of this test: John Carr (Iowa State University), Michael Mueterthies (Purdue University), and Phyllis Whittlesey (University of Alabama-Huntsville).

REFERENCES

- [1] C. Winslow, K. Bilger, and C. Baraona, "Space Station Freedom Solar Array Design Development," NASA TM-102105, 1989.
- [2] M. Cho, H. Masui, S. Iwai, T. Yoke, and K. Toyoda, "Three hundred fifty volt photovoltaic power generation in low earth orbit," *J. Spacecraft and Rockets*, Vol. 51, No. 1, pp. 379-381, Jan.-Feb. 2014.
- [3] M. Bodeau, "Current and Voltage Thresholds for Sustained Arcs in Power Systems," *IEEE-Trans. Plasma Science*, Vol. 40, No. 2, pp.192-200, Feb. 2012. doi: 10.1109/TPS.2011.2176932
- [4] K. H. Wright, Jr., T. A. Schneider, J. A. Vaughn, B. Hoang, V. V. Funderburk, F. Wong, and G. Gardiner, "Electrostatic Discharge Testing of Multi-Junction Solar Array Coupons after Combined Space Environmental Exposures," *IEEE-Trans. Plasma Sci.*, Vol. 40, No. 2, p. 334, Feb. 2012. doi: 10.1109/TPS.2011.2174447.
- [5] B. Hoang, F. Wong, R. Corey, G. Gardiner, V. V. Funderburk, R. Gahart, K. H. Wright, Jr., T. A. Schneider, and J. A. Vaughn, "Combined Space Environmental Exposure Tests of GaAs/Ge Solar Array Coupons," *IEEE-Trans. Plasma Sci.*, Vol. 40, No. 2, pp 324, Feb. 2012. doi: 10.1109/TPS.2011.2174161.
- [6] F. Wong, G. Gardiner, B. Hoang, T. Redick, R. Gahart, K. H. Wright, J. A. Vaughn, and T. A. Schneider, "Electrostatic Discharge Tests on Solar Array Wire Coupons Subjected to Simulated Space Environment Aging," *IEEE-Trans. Plasma Sci.*, Vol. 41, No. 12, pp 3359 – 3369, 2013. doi: 10.1109/TPS.2013.2277723
- [7] K. H. Wright, T. A. Schneider, J. A. Vaughn, B. Hoang, V. V. Funderburk, F. Wong, and G. Gardiner, "Age Induced Effects on ESD Characteristics of Solar Array Coupons After Combined Space Environmental Exposures," 12th Spacecraft Charging and Technology Conference, Kitakyushu, Japan, 14-18 May, 2012.
- [8] ISO-11221, "Space systems – Space solar panels – Spacecraft charging induced electrostatic discharge test methods," 2011.
- [9] B. Hoang, F. Wong, V. V. Funderburk, M. Cho, K. Toyoda, and H. Masui, "Electrostatic Discharge Test with Simulated Coverglass Flashover for Multi-Junction GaAs/Ge Solar Array Design," 35th IEEE Photovoltaic Specialists Conference (PVSC), pp 001118 – 001123, 20-25 June 2010. doi: 10.1109/PVSC.2010.5614721
- [10] D.C. Ferguson and B. V. Vayner, "Flashover Current Pulse Formation and the Perimeter Theory," *IEEE Trans. Plasma Sci.*, Vol. 41, No. 12, p.3393, Dec 2013.
- [11] J. M. Siguier, V. Inguibert, P. Sarrailh, D. Sarraill, G. Murat, J.-C. Matéo-Vélez, D. Payan, and N. Balcon, "Parametric study of a physical flashover simulator," *IEEE Trans. Plasma Sci.*, Vol. 40, No. 2, p. 311, Feb. 2012.
- [12] V. Inguibert, P. Sarrailh, J.-C. Matéo-Vélez, J.-M. Siguier, C. Baur, B. Boulanger, A. Gerhard, P. Pelissou, M. Sevoz, and D. Payan, "Measurements of the Flashover Expansion on a Real-Solar Panel – Preliminary Results of EMAGS3 Project", *IEEE Trans. Plasma Sci.*, Vol. 41, No. 12, p.3370, Dec 2013.
- [13] P. Sarrailh, V. Inguibert, J.-M. Siguier, J.-C. Matéo-Vélez, C. Baur, D. Payan, B. Boulanger, A. Gerhard, and P. Pelissou, "Plasma Bubble Expansion Model of the Flash-Over Current Collection on a Solar Array - Comparison to EMAGS3 Results", *IEEE Trans. Plasma Sci.*, Vol. 41, No. 12, p.3429, Dec 2013.
- [14] D.C. Ferguson et al., "A U.S. Round Robin Experiment on Characteristics of Arc Plasma Expansion," *AIAA 2012-2940*.
- [15] B. Vayner et al., "First Preliminary Results from U.S. Round-Robin Tests", *IEEE Trans. Plasma Sci.*, Vol. 41, No. 12, p.3310, Dec 2013.
- [16] J. A. Young, M. W. Crofton, D. C. Ferguson, R. C. Hoffmann, A. T. Wheelock, J. L. Prebola, D. H. Crider, K. Steele, J. J. Likar, T. A. Schneider, J. A. Vaughn, J. M. Bodeau, N. Noushkam, B. V. Vayner, S. Close, A. Goel, B. Hoang, "Preliminary Measurements of ESD Propagation on a Round Robin Coupon", 13th Spacecraft Charging and Technology Conference, Pasadena, CA, 23-27 June, 2014.
- [17] H. Masui, T. Ose, T. Kitamura, K. Toyoda, and M. Cho, "Characterization Experiments of Secondary Arcs on Solar Arrays: Threshold and Duration," *J. Spacecraft Rockets*, Vol. 47, No. 6, p. 966, Nov. – Dec. 2010.
- [18] T. Endo, T. Wada, H. Masui, K. Toyoda, and M. Cho, "Effect of Aging on Discharge Tolerance of Grouted Solar Array Panels Confirmed by Simulated Space Environment", 11th Spacecraft Charging and Technology Conference, Albuquerque, NM, 20-24 September, 2010.
- [19] B. Vayner, and J. T. Galofaro, "Inception and prevention of sustained discharges on solar arrays", *IEEE Transl. Plasma Science*, vol. 40, No. 2, pp. 388-393, Feb. 2012.
- [20] J.-M. Siguier, V. Inguibert, G. Murat, D. Payan, and N. Balcon, "Arcing test on an aged grouted solar cell coupon with a realistic flashover simulator", 13th Spacecraft Charging and Technology Conference, Pasadena, CA, 23-27 June, 2014.